Contactless Linear Rotary Joint at *Ku*-Band

Muhammad Tayyab Azim, Junhyeong Park, and Seong-Ook Park, *Member, IEEE*

***Abstract*— Our laboratory has developed a drone detection radar that involves a mechanical scanning antenna. Radar and antenna systems that have mechanical scanning require an additional component called a rotary joint (RJ). The purpose of RJ in scanning assemblies is to provide an uninterrupted link between the antenna and the transceiver. In our system, antenna and transceiver are linearly polarized and use TE_{10} mode along the rectangular waveguide section. TE_{10} modes are asymmetric in nature making them incompatible with the rotating motion of the antenna. An RJ is presented with back-to-back mode transitions using symmetric modes along the circular waveguide and contactless branch line joint. The mode used along the circular waveguide for symmetry purpose is TM_{01}. An I-type linear RJ topology is selected due to lack of space along the lateral directions and system configuration. The problem of antenna matching while scanning was solved at 14.0–14.5 GHz at *Ku*-band using single-channel linear RJ.**

***Index Terms*— Asymmetric and symmetric modes, circular waveguide modes, coaxial TEM mode and mode transition ridge waveguide, contactless joint.**

I. Introduction

THE antennas used in radar for scanning purposes are mostly mechanically steered, except for costly active electronic scanned arrays. In mechanical scanning, usually the antenna is rotated with a stationary transceiver. The device that allows antenna steering with a static transceiver is called rotary joint (RJ). In general, RJ has two parts: a stator and a rotor. The rotor part is connected with the scanning antenna and the stator part is connected with the transceiver, whereas the stator and rotor are connected to each other via rotary choke.

RJs have been designed using symmetric modes in circular or coaxial waveguides. In circular waveguides, a symmetric mode is excited with slots in the wall as reported in [1]. Input waveguide is divided with *H*-plane equal T power divider and coupled to a circular waveguide at opposite end through a slot. This kind of RJs requires sufficient radius of curvature for rectangular waveguide bend to minimize TE_{11} mode excitation. This is an effective technique but our radar system did not have enough lateral space to accommodate the bend. A similar design has been adopted and further improved to design dual-band RJ at *X*- and *Ka*-bands [2], using a nested coaxial-circular waveguide to provide the symmetric modes. A linear RJ at *Ku*-band with the minimum lateral space is designed using coaxial waveguide TEM mode [3]; however, coaxial waveguide limits the power handling capability of the RJ. The RJs in [1]–[3] use either TE_{10}-TM_{01} or TE_{10}-TEM mode conversion for rotation symmetry purpose. Kaiden *et al.* [4] have used circular polarized field and energy wave passes through the rotation section as TE_{11} mode. It is an H-shaped RJ with polarizers. Abramov *et al.* [5] have reported a U-style RJ with TM_{01} mode converter and right angle *E*-plane junction. Chang and Yu [6] have reported an RJ at 35 GHz with TE_{01} mode converter and details of the effect of gaps between the stator and the rotor.

Our drone detection radar requires a linear I-type RJ as less space is available in lateral directions due to system components. Scanning antenna and transceiver of our radar have WR-75 interface so the RJ with waveguide interface was required. I-type RJs are designed using coaxial waveguide, which are difficult to manufacture and require two joints one for the coaxial pin and one for the outer waveguide. In RJ, we have to make a mode conversion from asymmetric mode (TE_{10}) to symmetric mode. The first dominant mode in circular waveguides is TE_{11} which is asymmetric, TM_{01} and TE_{01} are the first symmetric modes in TM_{mn} and TE_{mn} categories, respectively. The mode converter used in our design is TM_{01} using a novel TEM-TM_{01} mode converter instead of TEM mode in I-type RJs with a single joint. The RJ is simply a mode converter from TE_{10}-TM_{01} along the stator, and TM_{01}-TE_{10} along the rotor. These two mode converters are joined together by a contactless joint which allows for a rotatory motion. A modular approach is followed in the design.

II. Design of Rotary Joint

The complete RJ is shown in Fig. 1. It has a stator and a rotor with a slight gap and contactless branch line joint. The rotor part is an exact mirror image of the stator in internal dimensions apart from the slight gap, which is mandatory for the contactless branch line coupler and rotation motion. The input of the rotor is a rectangular waveguide with standard WR-75 waveguide and TE_{10} input mode from the antenna. The design of RJ can be easily understood by a single-mode transition from TE_{10}-TM_{01} as shown in Fig. 1. The mode conversion in the rotor is a stepwise conversion from TE_{10} to TEM mode from rectangular waveguide to coaxial waveguide, followed by TEM to TM_{01} mode from coaxial waveguide to circular waveguide which completes the transition from asymmetric TE_{10} to symmetric TM_{01} modes. For rectangular-to-coaxial transition, we have used a tapered septum which is connected to the center pin of the coaxial waveguide

Manuscript received February 6, 2019; revised March 13, 2019; accepted April 13, 2019. Date of publication May 7, 2019; date of current version June 5, 2019. This work was supported by the Ministry of Land, Infrastructure and Transport of Korean Government through UAV Safety Technology Research Program under Grant 19ATRP-C108186-05. *(Corresponding author: Muhammad Tayyab Azim.)*

The authors are with the Microwave and Antenna Laboratory (MaLab), Korea Advanced Institute of Science and Technology (KAIST), Daejeon 34141, South Korea (e-mail: tayyabazim@kaist.ac.kr; bdsfh0820@kaist.ac.kr; soparky@kaist.ac.kr).

Color versions of one or more of the figures in this paper are available online at http://ieeexplore.ieee.org.

Digital Object Identifier 10.1109/LMWC.2019.2912271

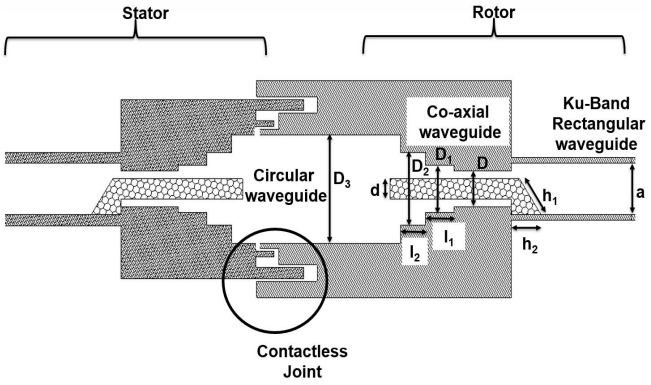

Fig. 1. Schematic of RJ model with appropriate waveguides and mode transitions.

as shown in Fig. 1. The transition is made for *Ku*-band at 14.0–14.5 GHz. The circular coaxial waveguide having air as a dielectric is used for TEM mode. The second part of transition consists of converting TEM mode to TM_{01} mode, i.e., converting from coaxial-to-circular waveguide. Finally, a contactless branch line joint is added between a stator and a rotor. The contactless joint is placed on the internal circular ring of bearing assembly, which provides a smooth rotary motion.

A. TE_{10}-TEM Transition

The first step is to convert the waveguide mode TE_{10} to TEM using septum ridge transition. The power flow and attenuation of coaxial are given by [7]

$$P = \frac{2\pi}{\ln(a/b)}\eta|V|^2 \tag{1}$$

$$\alpha = \left(\frac{R_a}{a} + \frac{R_b}{b}\right)\frac{1}{2\zeta \ln\left(\frac{a}{b}\right)} \tag{2}$$

where a and b are the outer and inner dimensions of the coaxial waveguide, respectively, η is the wave impedance $\sqrt{\mu_0/\epsilon_0}$, and ζ is $(1/\eta)$. R_a and R_b are the characteristic resistances of the outer and inner metals in coaxial waveguide. The maximum power flow in (1) is for a/b ratio of 1.65 (Z_{coax} 30 Ω), while minimum attenuation in (2) is for a/b ratio of 3.6 (Z_{coax} 70 Ω). For high-power application, (Z_{coax} 35.6 Ω) has been adopted, which is close to 30 Ω for power rating of the RJ with outer and inner conductor radii as 3.35 and 1.85 mm, respectively. The first higher order mode (TE_{11}) cutoff of coaxial waveguide with these dimensions is 18.37 GHz, which is well above our band of interest [8]. A transition from rectangular to coaxial is made with continuous linear impedance transformer using single ridge. The ridge end is connected to the center coaxial connector. As the coaxial connector center pin radius is 1.85 mm for 35.6 Ω, the ridge width is 3.7 mm so it connects directly with the coaxial connector. The ridge waveguide transformer has low impedance and f_c than a normal rectangular waveguide. Z_{VI} of ridge waveguide is calculated using analysis of [7], [9]

$$Z_{\text{VI}} = Z_{\text{VI}}(\infty)\frac{1}{\sqrt{1-\left(\lambda_{\text{air}}/\lambda_c'\right)^2}} \tag{3}$$

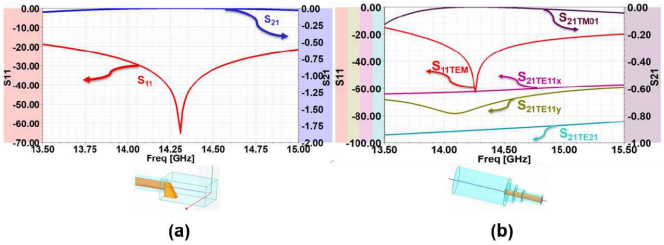

Fig. 2. (a) Rectangular waveguide to coaxial transition TE_{10}-TEM. (b) Coaxial-to-circular waveguide transition TEM-TM_{01}.

where Z_{VI} (∞) is calculated from [9]. As the ridge height is increased along h_1, the impedance of ridge section decreases and it serves as a linear impedance transformer from rectangular section to coaxial section. The ridge section apart from impedance transformer also acts as mode transformer between TE_{10} and TEM modes. The return loss and insertion loss of TE_{10}-TEM is shown in Fig. 2(a). The TE_{10}-TEM transition is concentric, i.e., the longitudinal axis of the coaxial and rectangular waveguide is the same. The guided wavelength in the ridge section increases as the ridge height decreases. The length h_2 in Fig. 1 of the septum is 6.2 mm The guided wavelength in the ridge waveguide can be calculated by [10]

$$\left(\frac{2\pi}{\lambda_g}\right)^2 = \left(\frac{2\pi}{\lambda_o}\right)^2 - \left(\frac{2\pi}{\lambda_c}\right)^2. \tag{4}$$

The cutoff wavelength for ridge waveguide can be calculated numerically, and with the help of (4), the guided wavelength can be estimated. The septum ridge was filet from the top to remove any sharp edges and discontinuities and provides a smooth transition from septum ridge to coaxial waveguide.

B. TEM-TM_{01}

For a transition from coaxial to circular, we need to select the mode along the circular waveguide. The lowest order cutoff mode of the circular waveguide is TE_{11} mode which is asymmetric and it cannot be used in RJ with linear polarization. The lowest order symmetric modes in TE_{mn} and TM_{mn} categories are TE_{01} and TM_{01} modes, respectively; however, f_{cTE01} is higher than f_{cTM01} because of root of Bessel function for TE_{mn} modes [7]. TM_{01} mode as symmetric mode for transition keeps a number of modes to a minimum along the waveguide and it can be excited in a linear transition from the coaxial waveguide. We can select the radius of circular waveguide greater than 8.2 mm to make f_{cTM01} mode cutoff frequency below our band of interest. However, a radius greater than 10 mm can also pass other higher modes in the waveguide if excited. We selected radius of 10 mm of the circular waveguide which makes f_{cTM01} as 11.48 GHz and f_{cTE21} as 14.58 GHz just above our band of interest.

The wave impedance for TM_{01} is given as $Z_{\text{TM01}} = (\lambda_0/\lambda_g)\eta$. The impedance of coaxial waveguide which will be launching TM_{01} mode in the circular waveguide is 35.6 Ω. For circular waveguide radius near 8 mm, the wave impedance Z_{TM01} will be small and matching might be considered as easier; however, the change in impedance due to frequency will be higher and impedance matching for a band of interest

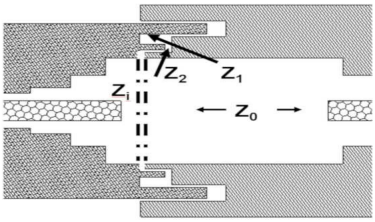

Fig. 3. Design of contactless joint.

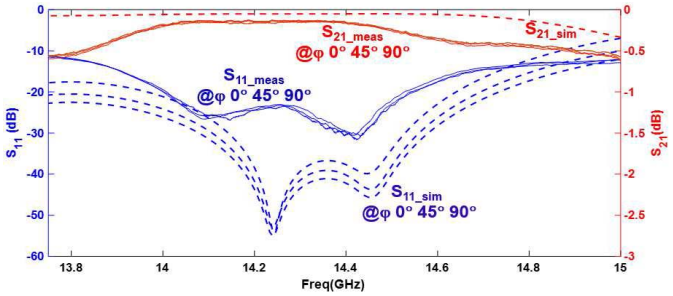

Fig. 4. Simulated and measured results.

will be a problem. Two-step impedance transformers are added before circular waveguide to cancel the discontinuity reflection in the structure. Since the steps are radially symmetric only TM_{0n} modes will be excited and as the circular waveguide can only pass TM_{01}, while TE_{11} excitation is kept minimum. As a result, TEM is converted to TM_{01} mode, from the power conservation condition in the structure. The results are shown in Fig. 2(b).

C. Contactless Joint Design

The two transitions are placed back to back with contactless joint and placed on the bearing to provide rotatory motion. The contactless joint configuration is shown in Fig. 3. Break in circular waveguide presents a discontinuity to the wave; however, if the input impedance of the joint Z_i can be controlled and minimized this gap will not impact the wave traveling inside the smooth circular waveguide. The joint is a series joint and has two chokes for impedance matching. The impedance of a short circuit at a distance of half wavelength is very close to zero. The length of the choke with Z_1 and Z_2 is $\lambda_0/4$ which provides a combined length of $\lambda_0/2$, a necessary condition for reducing Z_i. The chokes in the branch line make a coaxial waveguide and impedance of Z_2 and Z_1 can be controlled by the thickness of the choke. We have used Z_2 as 2.67 Ω and Z_1 as 8.9 Ω. The VSWR for the choke and its impact is calculated by [11]

$$\text{VSWR} = \left(\frac{Z_2}{Z_1}\right)\left(\frac{\pi\,\Delta\lambda}{2\lambda}\right)\left(1+\frac{Z_2}{Z_1}\right)+1. \tag{5}$$

From (5), it is observed that Z_2 should be very small to get a good standing-wave ratio (SWR) and return loss. However, too small Z_2 can make choke thickness very small so to make the choke structure practical a choke width as small as possible at the operating frequency is desired. The thickness of the second choke with Z_1 can be made a little thicker to satisfy (5).

III. Simulated and Measured Results

The two transitions TE_{10}-TEM and TEM-TM_{01} are connected in series to get TE_{10}-TM_{01} transition. This one transition constitutes the stator part. The same transition with a slight gap for the rotary choke and the same internal dimensions is used for the rotor part. The full-wave analysis of single-channel linear RJ is simulated with the help of commercial EM software by placing back to back two TE_{10} to TM_{01} transitions such that at input and output, we have TE_{10} modes, and at the center circular waveguide, we have TM_{01} mode. The S-parameters of the complete RJ at different rotation angles are shown in Fig. 4 with a good agreement between measured and simulated results. Table I gives a comparison among reported RJs. The RJ was measured using R&S ZNB 40 vector network analyzer and two standard WR-75 transitions. The Insertion loss was ≤0.2 dB from 14.0 to 14.5 GHz and ≤0.65 dB from 13.8 to 15 GHz.

TABLE I
Comparison Table

Model	Freq(GHZ)	IL(dB)	Topology
[2]	8.9-9.9	0.65	waveguide
[12]	11.6-12.6	1.09	SIW
[13]	13-15	1.2	waveguide
Presented	13.8-15	0.63	waveguide

IV. Conclusion

An I-type RJ with TM_{01} mode instead of TEM mode for drone detection radar was designed. The topology of RJ was different than topologies surveyed and reviewed due to the system requirement. Simulated and measured values were also in agreement. The approach of design presented in this letter can be extended to any frequency.

References

[1] D. G. de Mesquita and A. G. Bailey, "A symmetrically excited microwave rotary joint," *IEEE Trans. Microw. Theory Techn.*, vol. MTT-18, no. 9, pp. 654–656, Sep. 1970.
[2] A. Morini, "Design of a dual-band rotary joint operating in *x*- and *ka*-bands," *IEEE Trans. Microw. Theory Techn.*, vol. 59, no. 6, pp. 1461–1467, Jun. 2011.
[3] H. Torpi and S. M. Bostan, "Ku band rotary joint design for SNG vehicles," *Radioengineering*, vol. 24, no. 4, p. 913, Dec. 2015.
[4] M. Kaiden, K. Kimura, H. Ogawa, T. Kasuga, M. Tsuboi, and Y. Murata, "Septum polarizer for Ka-band H-shaped rotary joint," *J. Infr., Millim., THz. Waves*, vol. 30, no. 7, pp. 727–737, Jul. 2009.
[5] V. Abramov, H.-J. Park, D.-H. Kim, and T.-H. Lee, "U-style rotary joint with E_{01} mode for millimeter waves," in *IEEE MTT-S Int. Microw. Symp. Dig.*, vol. 3, Jun. 2004, pp. 1879–1882.
[6] T. H. Chang and B. R. Yu, "High-power millimeter-wave rotary joint," *Rev. Sci. Instrum.*, vol. 80, no. 3, Mar. 2009, Art. no. 034701.
[7] N. Marcuvitz, *Waveguide Handbook*, no. 21. London, U.K.: IET, 1951.
[8] D. M. Pozar, *Microwave Engineering*. Hoboken, NJ, USA: Wiley, 2012.
[9] T.-S. Chen, "Calculation of the parameters of ridge waveguides," *IRE Trans. Microw. Theory Techn.*, vol. 5, no. 1, pp. 12–17, Jan. 1957.
[10] J. Helszajn, *Ridge Waveguides and Passive Microwave Components*. London, U.K.: IET, 2001.
[11] D. Bin, Z. Hua-lin, and M.-C. Hu, "An analysis of circular waveguide rotary joint design with coupling TM_{01} mode," in *Proc. IEEE CIE Int. Conf. Radar*, vol. 2, Oct. 2011, pp. 1224–1227.
[12] Y. J. Cheng and Z. J. Xuan, "12-GHz rotary joint with substrate integrated waveguide feeder," *IEEE Trans. Microw. Theory Techn.*, vol. 64, no. 5, pp. 1508–1514, May 2016.
[13] S. Chakrabarty, V. K. Singh, and S. B. Sharma, "Dual frequency coaxial rotary joint with multi-stepped transition," *Int. J. Microw. Wireless Technol.*, vol. 2, no. 2, pp. 219–224, Jul. 2010.